Available online at www.sciencedirect.com
ScienceDirect
Cement and Concrete Research 38 (2008) 757–765
Cement and Concrete Research

Internal curing of high-performance concrete with pre-soaked fine lightweight aggregate for prevention of autogenous shrinkage cracking

Daniel Cusson *, Ted Hoogeveen

National Research Council Canada, Ottawa, Ontario, Canada K1A 0R6

Received 19 September 2007; accepted 8 February 2008

Abstract

The effectiveness of internal curing (IC) to reduce autogenous shrinkage cracking in high-performance concrete (HPC) was investigated using different levels of internal curing on four pairs of large-size prismatic HPC specimens tested simultaneously under free and restrained shrinkage. Internal curing was supplied by pre-soaked fine lightweight aggregate (LWA) as a partial replacement to regular sand. It was found that the use of 178 kg/m^3 of saturated LWA in HPC, providing 27 kg/m^3 of IC water, eliminated the tensile stress due to restrained autogenous shrinkage without compromising the early-age strength and elastic modulus of HPC. It was shown that the risk of concrete cracking could be conservatively estimated from the extent of free shrinkage strain occurring after the peak expansion strain that may develop at very early ages. Autogenous expansion, observed during the first day for high levels of internal curing, can significantly reduce the risk of cracking in concrete structures, as both the elastic and creep strains develop initially in compression, enabling the tensile strength to increase further before tensile stresses start to initiate later.

Keywords: Curing (*A*); High-performance concrete (*E*); Shrinkage (*C*); Creep (*C*); Mechanical properties (*C*)

1. Introduction

Proper curing of concrete structures is important to ensure they meet their intended performance and durability requirements. In conventional construction, this is achieved through external curing, applied after mixing, placing and finishing [1]. Internal curing (IC) is a very promising technique that can provide additional moisture in concrete for a more effective hydration of the cement and reduced self-desiccation [2]. Internal curing implies the introduction of a curing agent into concrete that will provide this additional moisture. Currently, there are two major methods available for internal curing of concrete. The first method uses saturated porous lightweight aggregate (LWA) [3] in order to supply an internal source of water, which can replace the water consumed by chemical shrinkage during cement hydration. This internal curing water is naturally drawn during cement hydration from the relatively large pores of the lightweight aggregate into the smaller pores of the cement paste. The second method uses super-absorbent polymers (SAP) [4], as these particles can absorb a very large quantity of water during concrete mixing and form large inclusions containing free water, thus preventing self-desiccation during cement hydration. For optimum performance, the internal curing agent should possess high water absorption capacity and high water desorption rates. The quantity of internal curing water required to replace the mix water consumed by chemical shrinkage can be easily estimated, as suggested elsewhere [5,6]. Detailed information on internal curing can be found in the new state-of-the-art report on internal curing of concrete from RILEM TC-196 [2].

Since the 1950's, internal curing had been inadvertently applied in lightweight concrete structures before its potential for reducing self-desiccation in high-performance concrete (HPC) structures was recognized later in the 1990's [7]. Lightweight aggregates were primarily used to reduce the weight of concrete structures; however, these aggregates were usually saturated prior to use in concrete to ensure adequate workability, since it was recognized that dry porous aggregates could absorb some of the mix water in fresh concrete [8]. These concrete structures

* Corresponding author.
E-mail address: Daniel.Cusson@nrc-cnrc.gc.ca (D. Cusson).

0008-8846/$ - see front matter.
doi:10.1016/j.cemconres.2008.02.001

were found to achieve long-term durability from their excellent in-service performance observed in the field [9,10]. More recently, lightweight aggregates have been used successfully in large construction projects for the purpose of internal curing of normal-density concrete structures. For example, in January 2005, about 190 000 m^3 of internally-cured concrete was used in a paving project in Hutchins, Texas, which was likely the largest project in the world taking advantage of internal curing with pre-soaked LWA [11]. Field observations reported marginal pavement cracking, and strength tests indicated that the 7-day flexural strengths reached 90% to 100% of the required 28-day flexural strength due to an improved hydration. They also found that the compressive strengths of air-cured cylinders were similar to those of wet-cured cylinders at all ages, suggesting that internally-cured concrete is less sensitive to poor external curing practices or unfavourable ambient conditions. Especially in low permeability concrete, conventional external curing may not be effective in preventing self-desiccation at the center of thick concrete elements. The use of internal curing, however, does not replace recommended curing practices, as it is important to keep the concrete surface continuously moist during the curing process in order to prevent surface cracking due to plastic or drying shrinkage in hot, dry or windy weather.

This paper presents experimental results from large-size prismatic internally-cured HPC specimens tested simultaneously under free and restrained autogenous shrinkage. The main objectives of this study are to determine the required level of internal curing needed to eliminate autogenous shrinkage in high-performance concrete, and to demonstrate that the risk of cracking in concrete structures under restrained conditions can be effectively reduced.

2. Experimental program

2.1. Materials

Four concrete mix designs were experimentally evaluated, including one reference concrete mix (Mix-0) with no internal curing, and three similar concrete mixes with different levels of internal curing, namely Mix-L, Mix-M and Mix-H with low, medium and high contents of pre-soaked LWA, respectively, as shown in Table 1. This was achieved by replacing part of the normal-density sand with pre-soaked lightweight aggregate sand. In this study, each concrete mix had 450 kg/m^3 of ASTM Type 1 cement, a total water–cement ratio of 0.34, and a cement–sand–coarse aggregate ratio of 1:2:2 by mass. The properties of the fine and coarse aggregates are provided in Table 2. The expanded shale lightweight aggregate sand used for internal curing had a dry-bulk density of 920 kg/m^3 and water content of 15% by mass of dry material. This LWA sand was slightly coarser than the normal-density sand, made of silica and quartz, and was in fact improving the particle size distribution of the aggregates in the concrete mix. As shown in Table 1, the quantities of LWA used in these mixes did not significantly affect the volumetric mass of concrete, which was 2410 kg/m^3 on average.

Table 1
Concrete mix formulations and fresh concrete properties

Constituent	Quantity			
	Mix-0	Mix-L	Mix-M	Mix-H
	(No IC)	(Low IC)	(Medium IC)	(High IC)
Total water (kg)	21.3	21.3	21.3	21.3
ASTM type 1 cement (kg)	62.5	62.5	62.5	62.5
Dry normal sand (kg)	125.0	117.5	110.0	100.0
LWA sand (kg, dry)	0.0	7.5	15.0	25.0
Dry coarse aggregate (kg)	125.0	125.0	125.0	125.0
Dry superplasticizer (kg)	2.1	2.5	2.1	2.7
Total *w/c*	0.34	0.34	0.34	0.34
Effective *w/c*	0.34	0.32	0.30	0.28
IC water/cement	0.00	0.02	0.04	0.06
LWA/total sand	0.00	0.06	0.12	0.20
Slump (mm)	215	210	140	102
Air content (%)	3.9	5.0	3.0	3.0
Volumetric mass (kg/m^3)	2428	2391	2420	2400

Table 2
Aggregate properties

Name	Type	Maximum size	Dry-bulk density	Fineness modulus	Water content
		(mm)	(kg/m^3)		(%)
Lightweight sand	Expanded shale	5	920	3.3	15
Regular sand	Silica, quartz	5	1650	2.6	0.3
Coarse aggregate	Limestone	20	1430	6.7	0.2

It is important to observe that the total amount of water (mix water and IC water) was kept the same in these concrete mixes, resulting in a constant total water–cement ratio of 0.34 for all mixes. Based on the mix water immediately available to fresh concrete before setting, the effective water–cement ratio ranged from 0.34 for the control concrete to 0.28 for the Mix-H concrete (Table 1). The goal of maintaining a constant total amount of water in the concrete mixes was twofold: (i) to prevent possible strength and stiffness reductions with more water and lightweight material in concrete, and (ii) to make the test more severe for internal curing as far as autogenous shrinkage is concerned, since concretes with lower water–cement ratios usually experience more severe self-desiccation.

The quantity of IC water needed to achieve maximum hydration in concrete was estimated from calculations based on the chemical shrinkage and maximum degree of hydration theoretically achievable in normal cement paste, as follows [2]:

$$\left(\frac{w}{c}\right)_{ic} = 0.18\left(\frac{w}{c}\right) \quad \text{for } w/c \le 0.36 \tag{1}$$

where $(w/c)_{ic}$ is the mass ratio of internal curing water to cement, and w/c is the mass ratio of mix water to cement. Using the effective w/c shown in Table 1, the theoretical quantities of internal curing water required to ensure maximum cement hydration were estimated at: 0.061 for Mix-0; 0.058 for Mix-L; 0.054 for Mix-M; and 0.050 for Mix-H. Since different levels of internal curing were desired in this study, lower than required quantities of IC water were provided in Mix-0, Mix-L and Mix-M. For the mix designs presented in Table 1, the percentage of IC water actually provided to that required in theory were: 0%

for Mix-0 (control); 34% for Mix-L; 74% for Mix-M; and 120% for Mix-H.

For each mix design, two large-size concrete specimens and additional small-size concrete samples were prepared from the same batch and sealed with plastic sheets to prevent external drying, since the focus of this study was on autogenous shrinkage prevention.

2.2. Testing procedures

A complete testing system and analysis method were previously developed for studying restrained shrinkage and tensile creep of large-size HPC specimens [12]. This approach, modified from existing approaches [13,14], presents new features including: (i) the use of large-size specimens, enabling the study of the mechanical behaviour of concrete made with large coarse aggregate and reinforcing bars; and (ii) the ability to impose a partial (or full) degree of restraint on the specimen through embedded reinforcing bars, which is representative of field conditions. An advantage of using a partial degree of restraint is that restrained shrinkage testing can be conducted without prematurely cracking those concrete specimens experiencing large shrinkage deformations (in our case the control specimen).

Fig. 1 presents the main setup used for testing free and restrained shrinkage of large-size prismatic concrete specimens (200 × 200 × 1000 mm). For each restrained specimen, the axial strain was measured with electrical strain gauges (SG) centered on four 10-mm reinforcing bars embedded in concrete. The test apparatus included a closed loop servo-hydraulic system to control the actuator using the rebar-mounted strain gauges as the feedback signal. The force, measured by a load cell, was transmitted to the concrete by the steel bars, which had their ends welded to the stiff end plates connected to the rigid test frame. For each concrete mix, an unrestrained companion specimen was prepared with no reinforcement. Free shrinkage was measured using LVDTs placed at both ends of the specimen. Two relative humidity (RH) sensors were placed in the unrestrained specimen to assess the extent of internal drying due to self-desiccation, and thermocouples (TC) were distributed in concrete as shown in Fig. 1. Detailed technical information on the test frame and test procedures is provided elsewhere [12].

Additional tests were simultaneously conducted on smaller concrete samples made of the same batch of concrete, including the determination of the thermal expansion coefficient on 75 × 75 × 295 mm prisms, as well as the compressive strength, splitting tensile strength and compressive modulus of elasticity on 100 × 200 mm cylinders. The temperature was monitored for each type of sample, and maturity (equivalent age at 25 °C) was calculated for each sample size in order to use consistent sets of results in the calculations. Maturity was calculated as follows [15]:

$$M(t) = \int_0^t \exp\left[\frac{E_a}{R}\left(\frac{1}{273 + T_{\text{ref}}} - \frac{1}{273 + T(t)}\right)\right] dt \qquad (2)$$

where t is the time after initial setting of concrete; E_a/R is the activation energy factor of the concrete (for which a value of 4000 K was experimentally determined [16]); T is the average concrete temperature as a function of time; and T_{ref} is the reference concrete temperature (taken here as 25 °C).

3. Results and analyses

3.1. Effect of internal curing on concrete temperature and relative humidity

During the free and restrained shrinkage experiments, the concrete specimens were tested under realistic temperature regimes, as shown in Fig. 2. Due to the heat produced by cement

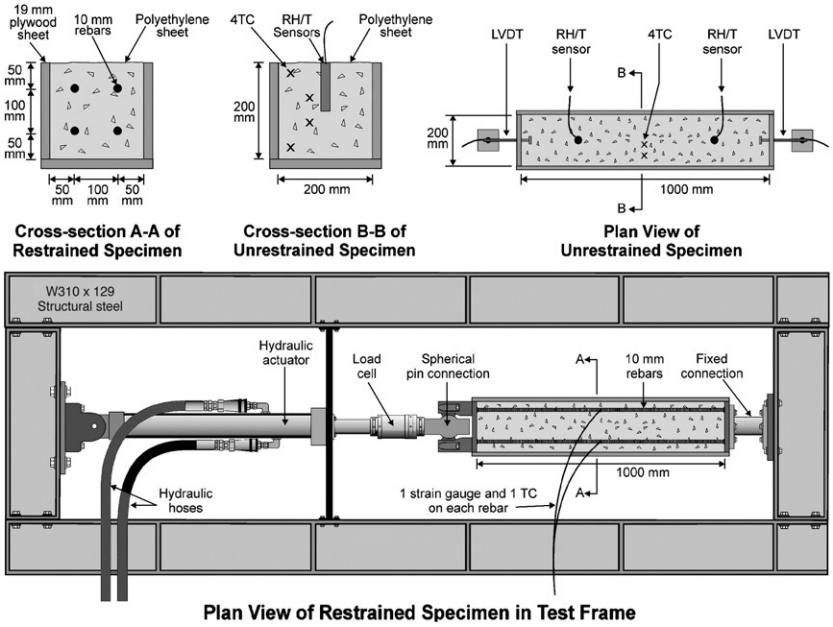

Fig. 1. Experimental setup for testing restrained and free shrinkage of large concrete specimens.

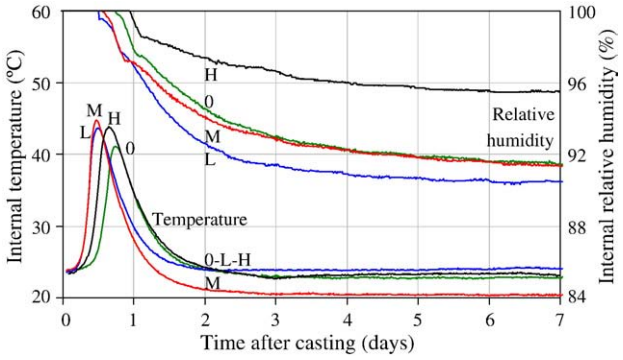

Fig. 2. Temperature and relative humidity measured in unrestrained concrete specimens.

hydration, the average concrete temperature reached 41 °C to 45 °C at 12 to 18 h after casting, depending on the specimen. After the cooling period, their average concrete temperature reduced to values between 21 °C and 24 °C near the age of 2 days, and remained constant thereafter (matching their respective ambient temperatures). It can be observed that when pre-soaked LWA sand is used for internal curing, the peak temperature is a few degrees higher and occurs a few hours earlier than for the control concrete with no LWA (sealed curing only), which may be due to the use of internal curing and a lower effective water–cement ratio.

Fig. 2 also presents the relative humidity measured in these concrete specimens (each curve is an average from two distinct sensors). For the control specimen (sealed curing only), the RH decreased from 100% initially to 94% after 2 days and to 92% after 7 days. However, when a low level of internal curing was used (Mix-L specimen), the concrete RH was approximately 2% lower than in the control specimen at any given time. With further increases in the quantity of LWA used for internal curing (from Mix-L to Mix-H), the RH remained relatively higher in concrete, with an RH of 98% after 2 days and 96% after 7 days, which are well beyond the RH values measured in the control specimen at these times.

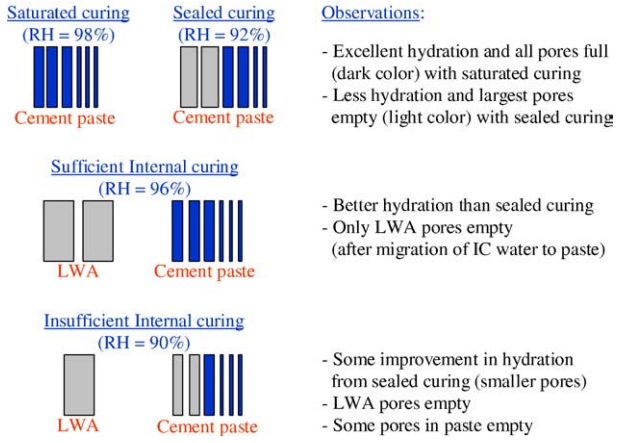

Fig. 3. Conceptual representation of cement paste pore systems under different curing conditions (modified from [17]).

Fig. 3 (modified from [17]) gives a conceptual illustration of different pore systems in cement paste under various curing conditions. It may be used to explain the reduced relative humidity measured in Mix-L concrete (insufficient internal curing) compared to Mix-0 concrete (sealed curing only). In the case of insufficient internal curing, hydration may have improved from sealed curing (with some reduction in pore sizes), however, all pores in LWA and some pores in the cement paste may be left empty after the small quantity of internal curing water is consumed by the cement hydration reaction, thus resulting in slightly lower RH in the system. In Fig. 3, the case of sufficient internal curing likely represents Mix-H concrete, in which all pores in the cement paste are filled with water while the pores in LWA are empty after migration of IC water to the cement paste.

3.2. Effect of internal curing on free shrinkage strain

Fig. 4 presents the total strain measured in the unrestrained concrete specimens for 7 days. This measurement includes free autogenous shrinkage and thermal strains (drying shrinkage prevented). Note that in this paper, negative strain values represent a contraction (shrinkage) and positive strain values represent an expansion. It can be readily seen that the addition of pre-soaked LWA for internal curing allowed early-age expansion to occur, which was due to autogenous swelling and thermal expansion, with peaks observed between 8 and 12 h of age. The extent of expansion increased with the quantity of pre-soaked LWA used in the concrete mix. Mix-H was the only concrete producing positive values of total strain after the first day until the end of testing at 7 days.

The thermal strain was calculated from the average concrete temperature measured in each concrete specimen as a function of time (Fig. 2) and the coefficient of thermal expansion (CTE) determined on smaller concrete prisms (75 × 75 × 295 mm). The equipment and procedures used for testing the CTE is described elsewhere [18], where it was found that: (i) CTE increases from a low value of 8×10^{-6}/°C shortly after setting to a maximum value of 11×10^{-6}/°C after 10 days, and (ii) the use of internal curing did not affect the early-age CTE of concrete compared to sealed-cured concrete. Calibrated on experimental results [18], the following empirical model for thermal expansion

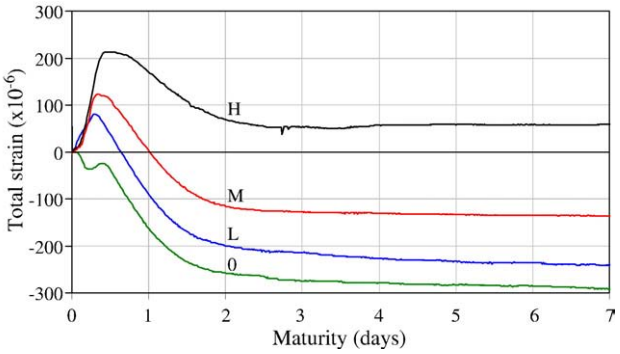

Fig. 4. Total strain measured in unrestrained concrete specimens.

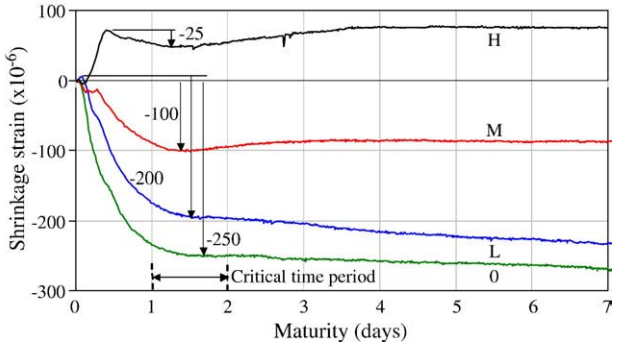

Fig. 5. Autogenous shrinkage strain measured in unrestrained concrete specimens.

was therefore determined for the concrete used in the present study:

$$\alpha_c(t) = 8 + 1.3\mathrm{LN}(t) \quad \text{ensuring that} \quad 8\times10^{-6}/°\mathrm{C} \le \alpha_c \le 11\times10^{-6}/°\mathrm{C} \tag{3}$$

where α_c is the concrete CTE determined as a function of time t after setting (days).

The autogenous shrinkage strain was thus determined by subtracting the calculated thermal strain from the total strain measured in the unrestrained specimen, and is presented in Fig. 5 for each concrete specimen. It can be seen that most of the autogenous deformations occurred within 24 to 48 h, with only limited changes thereafter. This observation emphasizes an important requirement for the prevention of autogenous shrinkage in concrete structures: shrinkage prevention measures must be effective shortly after setting of concrete before significant tensile stresses develop in concrete during the cooling period. For each concrete specimen, a critical strain value of net autogenous shrinkage was calculated at around 36 h of age which, in each case, corresponded to the time with the highest net shrinkage strain to tensile strength ratio. These critical net shrinkage strains ranged from only -25×10^{-6} for Mix-H concrete to a much larger value of -250×10^{-6} for Mix-0 concrete. It should be noted that Mix-L concrete, which only had 6% LWA sand (relative to the total mass of sand), experienced 20% less shrinkage than the control concrete (from -250×10^{-6} to -200×10^{-6}).

3.3. Effect of internal curing on restrained shrinkage stress

Stress calculations based on preliminary shrinkage testing indicated a high risk of cracking in Mix-0 concrete specimen if tested under full restraint (i.e. zero displacement). It was therefore decided to test the restrained specimens under a partial restraint of 0.9 (i.e. allowing only 10% of total shrinkage to take place), thus slightly reducing the tensile stresses developing in the restrained specimens. Fig. 6 presents the degree of restraint applied to each restrained concrete specimen during the 7-day period of testing, which was defined as:

$$K(t) = 1 - \frac{\varepsilon^R_{\mathrm{tot}}(t)}{\varepsilon^F_{\mathrm{tot}}(t)} \tag{4}$$

where $\varepsilon^R_{\mathrm{tot}}$ is the total strain allowed in the restrained concrete specimen (depending on the preset degree of restraint); and $\varepsilon^F_{\mathrm{tot}}$ is the total strain measured in the free (unrestrained) companion specimen.

For Mix-0, Mix-L and Mix-M specimens, the target value of 0.9 was difficult to maintain during the first day of testing, at which time the concrete specimen expanded or contracted very rapidly. The high relaxation of concrete at very early age prevented any cracking in the specimens. For Mix-H specimen, the applied degree of restraint was temporarily slightly over 1.0 during the first 3 days (i.e. the loading system was actually pulling on the specimen), however, this caused no problem since Mix-H concrete had very small autogenous shrinkage deformations and high relaxation resulting in relatively low tensile stresses developing in concrete.

Fig. 7 illustrates the tensile stress developing over time in each restrained concrete specimen. It can be observed that Mix-M and Mix-H specimens first experienced restrained expansion resulting in compressive stresses during the first day, followed by tensile stresses developing in the specimens due to restrained shrinkage. It is clear that the high level of internal curing in Mix-H specimen resulted in smaller tensile stresses compared to the other concrete specimens, even if Mix-H specimen was tested under a somewhat higher degree of restraint (see Fig. 6). It should be emphasized that most of the tensile stresses produced in Mix-H concrete specimen was actually not due to restrained autogenous shrinkage but to restrained thermal contraction

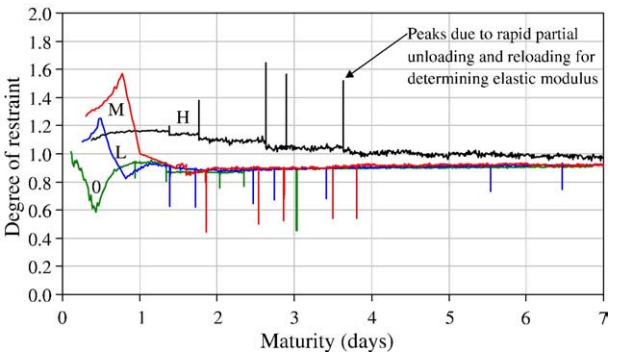

Fig. 6. Degree of restraint imposed on restrained concrete specimens.

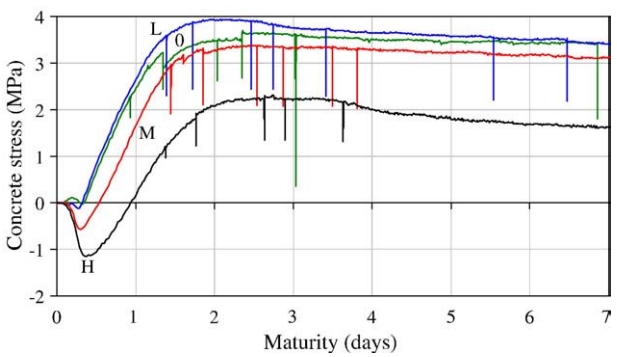

Fig. 7. Concrete stress measured in restrained concrete specimens.

during the cooling period. As shown in Fig. 5, it is recalled that the critical net autogenous shrinkage strain was rather small in Mix-H specimen compared to its thermal contraction strain, of which the extent may be assessed from Fig. 4.

3.4. Effect of internal curing on risk of concrete cracking

Conventional concrete starts shrinking near the time of initial setting, from which time shrinkage should be measured experimentally since, in actual concrete structures, tensile stresses will start to develop around that time if movement is restrained. In this case, all of the shrinkage strain will be responsible for the development of tensile stresses, depending on the visco-elastic properties of concrete. In structures made with concrete that may experience swelling at early ages, not all of the strain will produce tensile stresses if movement is restrained, as some of it will generate compressive stresses initially (as previously shown in Fig. 7). In that particular case, when testing free shrinkage of concrete specimens to assess the potential risk of cracking in concrete structures, large underestimations may occur if the extent of shrinkage strain used to evaluate that risk is determined from the time of setting.

To illustrate this point, Fig. 8 presents the development of the total strain (i.e. thermal+autogenous shrinkage strains) measured in the unrestrained Mix-H concrete specimen (from Fig. 4) and the development of the corresponding concrete stress measured in the companion specimen under restraint (from Fig. 7). It is clearly shown that, although the measured total strain always remained positive (absolute expansion), the tensile stress in the concrete specimen reached a value of 2 MPa in only 2 days. This is due to the fact that the beneficial expansion occurred when the modulus of elasticity was relatively small and the effect of creep was relatively large at very early ages, resulting in a low peak compressive stress (−1 MPa), followed later by restrained thermal contraction with an increased modulus of elasticity and reduced creep resulting in the development of tensile stress.

Ideally, the extent of shrinkage strain to consider when evaluating the risk of cracking in concrete structures should be the amount of strain developing after the time at which compressive stresses reverse into tensile stresses (i.e. after $\varepsilon_{\sigma=0}$). For the data in Fig. 8, an ideal net shrinkage strain of -125×10^{-6} ($\varepsilon_{min}-\varepsilon_{\sigma=0}$) would be obtained at 3 days, which is more

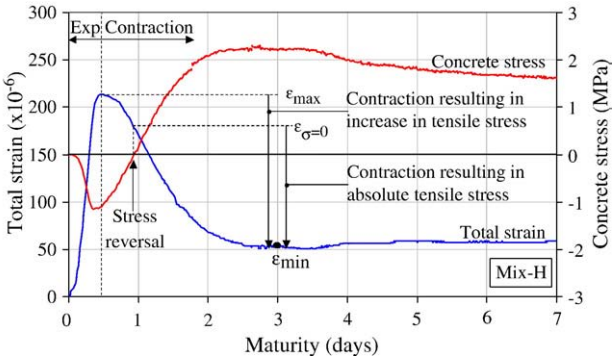

Fig. 8. Total strain and resulting stress in Mix-H concrete specimens.

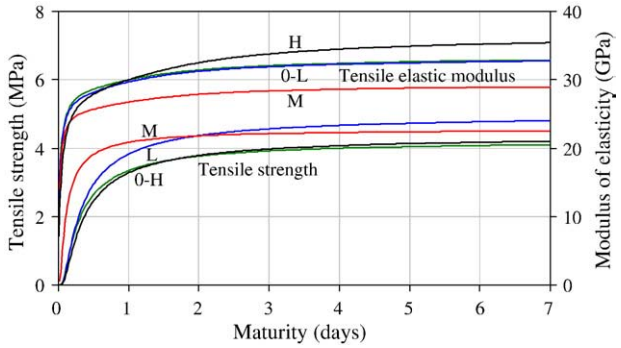

Fig. 9. Tensile strength and modulus of elasticity measured for different concrete mixes.

meaningful than the absolute value of $+50\times10^{-6}$ at 3 days. However, when testing shrinkage under a stress-free condition, such information ($\varepsilon_{\sigma=0}$) is not available. In this case, it is suggested to rely on the extent of free shrinkage strain (or net shrinkage strain) occurring after the peak of expansion (i.e. after ε_{max}), which would result in a conservative assessment of the risk of cracking in concrete structures. The net shrinkage strain was calculated as follows:

$$\varepsilon_{sh\ net}(t) = \varepsilon_{sh}(t) - \varepsilon_{exp\ max} \quad (5)$$

where $\varepsilon_{sh}(t)$ is the shrinkage strain measured as a function of time after initial setting; $\varepsilon_{exp\ max}$ is the peak strain value of the autogenous expansion, if any ($\varepsilon_{exp\ max}=0$ if no expansion).

From Fig. 8, the critical value of net shrinkage strain would be -160×10^{-6} (i.e. $\varepsilon_{min}-\varepsilon_{max}$) at 3 days, which is actually the extent of shrinkage strain contributing to the increase in tensile stress in the restrained concrete specimen. This proposed definition of net shrinkage has the double advantage of being conservative and independent of the choice of Time Zero in shrinkage testing [19]. Whether Time Zero is defined as 'time after casting', 'time after setting' (preferred), or 'time after peak of expansion', the critical or ultimate value of net shrinkage strain according to Eq. (5) will always remain unaffected.

The risk of cracking in concrete structures also depends on the rates at which tensile strength and modulus of elasticity develop (as illustrated in Fig. 9). The tensile strength curves were determined by linear regression of splitting tensile strength

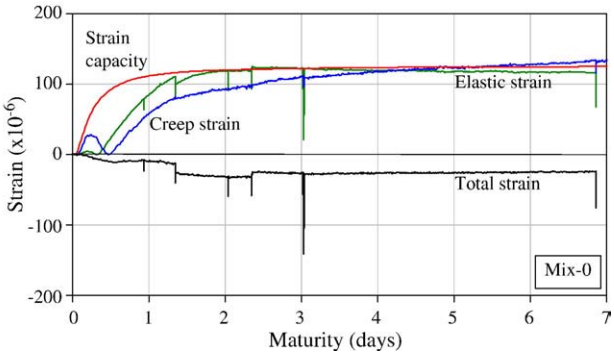

Fig. 10. Total, creep and elastic strains obtained for restrained Mix-0 concrete specimen.

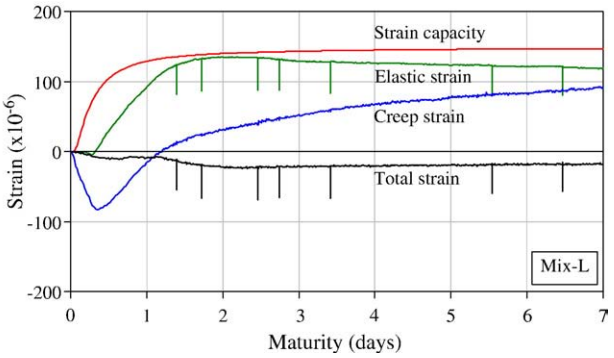

Fig. 11. Total, creep and elastic strains obtained for restrained Mix-L concrete specimen.

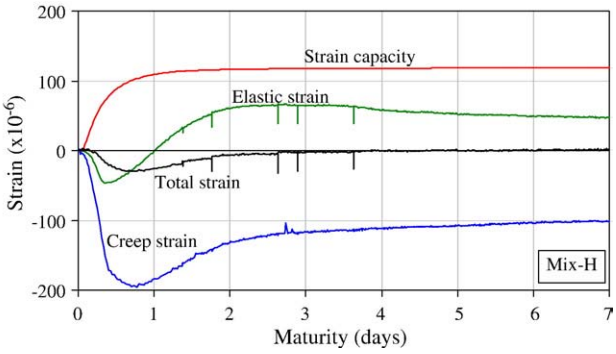

Fig. 13. Total, creep and elastic strains obtained for restrained Mix-H concrete specimen.

test results obtained at 1, 2, 4, 7 and 28 days on 100×200 mm concrete cylinders (tested in triplicates). The curves for the tensile modulus of elasticity were determined by linear regression of modulus values obtained at various times. These values were first determined from stress–strain data obtained during rapid partial unloading/reloading cycles conducted on the large-size concrete specimens during the restrained shrinkage experiments (vertical lines in Fig. 7). The curves shown in Fig. 9 provide no indication that internal curing compromises the development of either tensile strength or modulus of elasticity until an age of 7 days.

3.5. Effect of internal curing on creep and elastic strains

Figs. 10–13 present the creep and elastic strains as well as the total strain and strain capacity calculated for each of the four concrete specimens tested under restrained shrinkage. The strain analysis was based on compatibility of strain:

$$\varepsilon_{tot}(t) = \varepsilon_{el}(t) + \varepsilon_{cr}(t) + \varepsilon_{sh}(t) + \varepsilon_{th}(t) \quad (6)$$

where ε_{tot} is the total strain allowed in the restrained concrete specimen measured as a function of time t; ε_{el} is the elastic strain calculated by dividing the measured concrete stress (Fig. 7) by the corresponding tensile modulus of elasticity (Fig. 9) developing in the restrained specimen; ε_{cr} is the creep strain of concrete; and $\varepsilon_{sh}+\varepsilon_{th}$ are the shrinkage and thermal strains measured together (Fig. 4) in the unrestrained concrete specimen

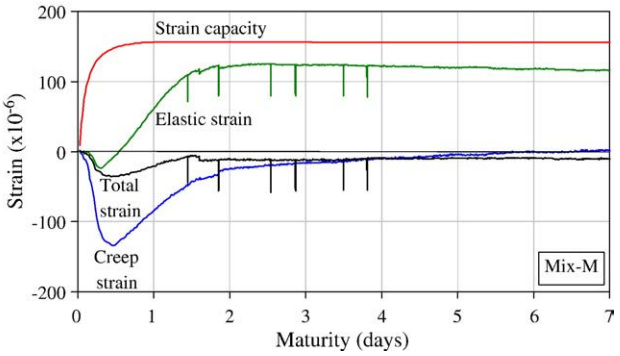

Fig. 12. Total, creep and elastic strains obtained for restrained Mix-M concrete specimen.

(with a small correction to account for the internal restraint provided by the reinforcement in the restrained concrete specimen [12]). Finally, the strain capacity presented in Figs. 10–13 was calculated by dividing the concrete tensile strength (Fig. 9) by the corresponding tensile modulus of elasticity (Fig. 9).

In Fig. 10 for the control concrete specimen with no internal curing, it can be seen that the elastic strain came very close to the strain capacity at an age of 1.5 days. It is clear that under full restraint ($K=1.0$), this specimen would have cracked, which would have ended the test prematurely. Similar behaviour and conclusion also apply to Mix-L concrete specimen in Fig. 11, where the elastic strain almost reached the tensile strain capacity at an age of 1.5 days for a degree of restraint near 0.9. On the other hand, with higher levels of internal curing Mix-M and Mix-H concrete specimens performed quite well (Figs. 12 and 13, respectively), with the elastic strain always lower than the strain capacity at any given time. Note that most of the elastic strain development was due to thermal contractions during the cooling period. For these two concrete specimens with restrained expansion in the first day (before cooling), the elastic strain went into the compressive range allowing the strain capacity to develop further by the time the elastic strain reversed into the tensile range, which actually reduced the risk of cracking.

The creep strain also developed differently depending on the extent of restrained expansion occurring in the concrete specimens at early age. With an increased quantity of pre-soaked LWA used in the specimens, larger creep strains developed in compression due to more significant restrained expansion. During the cooling period and after, increments of tensile creep strain developed due to restrained contraction resulting in a reduction in compressive creep strain towards the tensile range. Regardless of the concrete mixes tested, it is clear from these curves that creep developed very rapidly during the first day with a gradually decreasing development rate thereafter, as typically expected with normal concrete under load.

4. Effectiveness of internal curing

4.1. Effectiveness in shrinkage reduction

Fig. 14 illustrates the effectiveness of the LWA used for internal curing in reducing autogenous shrinkage of the concrete mixes tested in this study. It is shown that the reduction in the

critical strain value of net autogenous shrinkage (Fig. 5) is approximately proportional to the quantity of internal curing water provided in concrete by the LWA. This curve indicates that the optimum $(w/c)_{ic}$ for these concrete mixes would be 0.067 in order to reduce to zero the critical value of net shrinkage strain. This optimum ratio, however, is valid for the specific concrete mixes and LWA (15% water absorption) used in this study, and does not account for external drying shrinkage and thermal effects that may superpose on autogenous shrinkage in actual concrete structures. It may not be recommended to exceed this limit unless further testing is conducted, since some adverse effects might occur, such as a possible strength and stiffness reductions and excessive autogenous swelling. Detailed information on the benefits and possible adverse effects of internal curing can be found in [2].

4.2. Effectiveness in strength and stiffness enhancement

A great concern for design engineers and contractors is whether concrete structures will achieve the specified compressive strength and durability requirements in service. It has been clearly shown in this paper and elsewhere [2] that internal curing can eliminate the tensile stress due to net autogenous shrinkage. However, it has been also observed in some cases [20] that concrete made with saturated LWA may have slightly lower strengths at early age, due to an increased water-entrained porosity.

The test results presented in Table 3, however, show that sufficient internal curing can considerably reduce autogenous shrinkage without affecting the strength and stiffness of concrete measured at 7 days on 100×200 mm concrete cylinders. As explained earlier, this was achieved by reducing the amount of mix water in the concrete by an amount equal to that used for internal curing, thus reducing the effective mix water–cement ratio. As a result, the 7-day strength and elastic modulus were not reduced. An increased dosage of superplasticizer is therefore recommended in this case to achieve adequate workability. Other studies [21,22], however, have shown that the compressive strength can be improved by adequate internal curing without having to reduce the effective water–cement ratio.

It may be observed in Table 3 that the values of compressive modulus of elasticity differ slightly from those determined during the restrained shrinkage experiments at 7 days (Fig. 9).

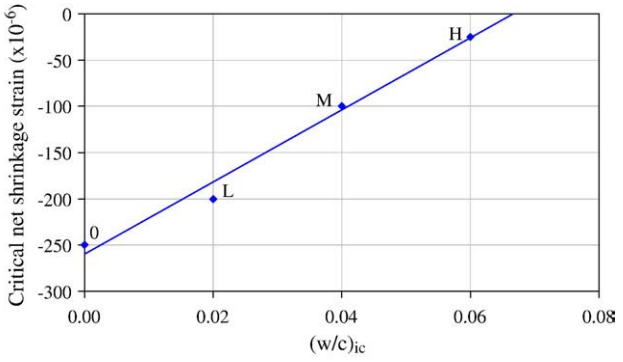

Fig. 14. Critical net shrinkage strain as a function of IC water–cement ratio.

Table 3
Hardened concrete properties measured at 7 days

Concrete mix ID	Splitting tensile strength	Compressive strength	Compressive modulus of elasticity	Critical value of net autogenous shrinkage
	(MPa)	(MPa)	(GPa)	($\times 10^{-6}$)
Mix-0	4.1	50	31.6	−250
Mix-L	4.8	50	31.2	−200
Mix-M	4.5	54	32.0	−100
Mix-H	4.2	57	31.4	−25

These differences may be due to different factors such as: stress type, specimen size, and specimen geometry, since the tensile modulus of elasticity was tested on large-size prismatic specimens (200×200×1000 mm) and the compressive modulus of elasticity was tested on smaller-size cylindrical specimens (100×200 mm).

5. Summary and conclusions

This study demonstrated an effective approach for reducing cracking due to autogenous shrinkage in high-performance concrete (HPC) structures. Free and restrained shrinkage testing of large-size HPC specimens was conducted under sealed condition to study the effect of internal curing on the structural performance of normal-density HPC specimens. The following conclusions were drawn:

1. The risk of concrete cracking can be conservatively estimated from the extent of shrinkage strain occurring after the peak expansion strain that may develop at early age. This net shrinkage strain can be simply determined from free shrinkage testing, and has the advantage of being independent of the onset of strain measurement.
2. Autogenous shrinkage of HPC, if not controlled, can reach high strain values within only 24 h (e.g. -250×10^{-6} for the reference specimen), leading to premature cracking if movement is fully restrained. The period between 24 and 48 h after setting was considered critical, at which time the highest tensile stress/strength ratios were measured. This means that adequate autogenous shrinkage prevention measures must be active at very early ages.
3. Mix-H concrete with $(w/c)_{ic}=0.06$ provided adequate internal curing with high relative humidity in the concrete (RH of 96% at 7 days), which is close to that usually provided by saturated curing (98%). However, Mix-L concrete with $(w/c)_{ic}=0.02$ provided insufficient internal curing with a 7-day RH of 90%, compared to 92% for the control concrete specimen with sealed curing only.
4. The internal curing water supplied in Mix-H concrete with $(w/c)_{ic}=0.06$ was able to eliminate autogenous shrinkage almost completely, and to maintain the critical tensile stress well under the tensile strength. It was shown in this case that most of the residual tensile stress in concrete was due to restrained thermal contraction, not autogenous shrinkage.
5. The quantities of pre-soaked LWA sand used in the concrete specimens (up to 178 kg/m^3) did not adversely affect the

strength and elastic modulus of concrete at 7 days. This was achieved by reducing the mix water by the amount of IC water contained in the LWA (up to 27 kg/m^3).

6. Autogenous swelling was observed within the first day for the specimens using pre-soaked LWA for internal curing, resulting in beneficial compressive stresses. The swelling strain increased (up to $+200\times10^{-6}$) with an increase in the mass of saturated LWA used in the mix.
7. The visco-elastic behaviour of the concrete specimens changed according to the extent of restrained expansion produced before cooling. As both the elastic and creep strains initially developed in compression with high levels of internal curing, the concrete tensile strength had more time to develop before the tensile stress started to initiate later, thus reducing considerably the risk of cracking of HPC.

Acknowledgments

The authors would like to thank Mr. John Roberts of Northeast Solite Corporation (Saugerties, NY) for providing the lightweight aggregate, as well as Dr. Lyndon Mitchell and Mr. Glendon Pye of NRC for their scientific input and technical assistance.

References

[1] ACI 308R, "Guide to curing concrete", American Concrete Institute, Farmington Hills, USA, Michigan, 2001 31 pp.
[2] RILEM TC-196, Internal curing of concrete, state-of-the-art report of RILEM technical committee 196-ICC, in: K. Kovler, O.M. Jensen (Eds.), RILEM Publications S.A.R.L. France, Bagneux, 2007, 139 pp.
[3] S. Weber, H.W. Reinhardt, A new generation of high performance concrete: concrete with autogenous curing, Advanced Cement Based Materials 6 (2) (1997) 59–68.
[4] O.M. Jensen, P.F. Hansen, Water-entrained cement-based materials: I. Principle and theoretical background, Cement and Concrete Research 31 (4) (2001) 647–654.
[5] S. Zhutovsky, K. Kovler, A. Bentur, Influence of cement paste matrix properties on autogenous curing of high-performance concrete, Cement & Concrete Composites 26 (2004) 499–507.
[6] D.P. Bentz, P. Lura, J.W. Roberts, Mixture proportioning for internal curing, Concrete International (February 2005) 1–6.
[7] R.E. Philleo, Concrete science and reality, in: J.P. Skalny, S. Mindess (Eds.), Materials Science of Concrete II, American Ceramic Society, Westerville, USA, 1991, pp. 1–8.
[8] ACI 213R, Guide for structural lightweight-aggregate concrete, American Concrete Institute, Farmington Hills, USA, 2003, 38 pp.
[9] T.A. Holm, T.W. Bremner, State-of-the-art-report on high-strength, high-durability structural low-density concrete for applications in severe marine environments, U.S. Army Corps of Engineers, Report No. ERDC/SL TR-00-3, August 2000, 116 pp.
[10] J.W. Roberts, B. Jones, J. Hulsman, Improving the durability and economy of short and medium span bridges through internal curing, 7th International Conference on Short and Medium Span Bridges, Montreal, Canada, August 2006, 10 pp.
[11] V.H. Villarreal, D.A. Crocker, Better pavements through internal hydration, Concrete International (February 2007) 32–36.
[12] D. Cusson, T. Hoogeveen, An experimental approach for the analysis of early-age behaviour of high-performance concrete structures under restrained shrinkage, Cement and Concrete Research 37 (2) (February 2007) 200–209.
[13] K. Kovler, Testing system for determining the mechanical behaviour of early-age concrete under restrained & free uniaxial shrinkage, Materials & Structures 27 (1994) 324–330.
[14] O. Bjontegaard, T. Kanstad, E.J. Sellevold, T.A. Hammer, Stress inducing deformations and mechanical properties of high-performance concrete at very-early-ages, 5th Int. Symposium on Utilization of High-Strength/High-Performance Concrete, Norway, Sandefjord, June 1999, pp. 1027–1040.
[15] P.F. Hansen, E.J. Pedersen, Maturity computer for controlled curing and hardening of concrete, Nordisk Betong 41 (19) (1977) 21–25.
[16] J. Zhang, D. Cusson, L. Mitchell, T. Hoogeveen, J. Margeson, The maturity approach for predicting different properties of high-performance concrete, 7th International Symposium on Utilization of High-Strength/High-Performance Concrete, Washington, USA, ACI SP 228-11, 1, June 20–24, 2005, pp. 135–154.
[17] D. Bentz, P. Halleck, A. Grader, J. Roberts, Four-dimensional X-ray microtomography study of water movement during internal curing, Slide Presentation made at the International RILEM conference on Volume Changes of Hardening Concrete: Testing and Mitigation, August 20–23, 2006, Denmark, Lyngby.
[18] D. Cusson, T. Hoogeveen, New test method for determining coefficient of thermal expansion at early age in high-performance concrete, 12th International Conference on Chemistry of Cement, Montreal, Canada, July 2007, 12 pp.
[19] A. Bentur, Early age cracking tests, in early age cracking in cementitious systems, report of RILEM committee TC 181-EAS, in: A. Bentur (Ed.), RILEM Publications Sarl, France, Bagneux, 2002, pp. 241–255.
[20] S. Zhutovsky, K. Kovler, A. Bentur, Influence of cement paste matrix properties on the autogenous curing of high-performance concrete, Cement and Concrete Composites 26 (2004).
[21] D.P. Bentz, Internal curing of high-performance blended cement mortars, ACI Materials Journal 104 (4) (July–August 2007) 408–414.
[22] D. Cusson, Effect of blended cements on efficiency of internal curing of HPC, ACI-SP, Internal Curing of High-Performance Concretes: Laboratory and Field Experiences, American Concrete Institute, Farmington Hill, MI, October 2007 15 pp.